06,11,19

Influence of sintering temperature on grain size and electrocaloric effect of barium titanate ceramics

© I.A. Starkov[1], A.S. Anokhin[1,2], I.L. Mylnikov[1,2], M.A. Mishnev[1], A.S. Starkov[1,2]

[1] St. Petersburg State Electrotechnical University „LETI",
St. Petersburg, Russia
[2] ITMO University,
St. Petersburg, Russia

E-mail: ferroelectrics@ya.ru

Received September 21, 2021
Revised December 3, 2021
Accepted December 6, 2021

A theoretical study of the polarization distribution and mechanical stresses in a ferroelectric ball located in an unlimited dielectric space has been carried out. The ball is covered with a dielectric and air shell. The external electric field far from the ball is assumed to be uniform. The polarization in the ball satisfies the nonlinear Landau–Ginzburg equation, which takes into account the presence of electrostriction. It is also assumed that for a small ball, the effect of local elastic stresses on polarization can be replaced by their homogenized value over the volume of the ball. Under this assumption, the distribution of the stress and the electric field can be obtained both in the ball and outside it. The dependence of the Curie–Weiss temperature on the radius of the ball is derived. The resulting solution is used to simulate the properties of microgranular ceramics. Along with the developed theoretical model, a series of experiments was carried out to measure the temperature dependence dielectric constant and the electrocaloric effect (ECE) for $BaTiO_3$ ceramics synthesized at different temperatures. The change in temperature during ECE was measured by direct methods. The greatest value of the ECE was achieved for ceramics synthesized at 1350°C. The magnitude of the change in temperature with a change in the electric field by 2 mV/m was $\Delta T = 0.42$ K. The observed experimental results demonstrate the possibility of using the theoretical four-phase model of ceramics to predict the dependence of the properties of ceramics on the sintering temperature.

Keywords: ferroelectrics, electrocaloric effect, barium titanate ($BaTiO_3$), granular media, sintering temperature, grain size.

DOI: 10.21883/PSS.2022.04.53499.208

1. Introduction

Ceramic ferroelectric films and multilayered structures on their basis attract close attention thanks to the possibilities of their wide application in the creation of a new generation of memory devices, capacitors, pyroelectric detectors etc. (see, for instance, [1]). In recent years, the sphere of application of such materials has extended due to the use in solid-state cooling devices [2,3] based on the electrocaloric effect (ECE). It is to be recalled that ECE means a reversible change of sample's thermal properties (temperature, entropy, heat capacity) upon a change in electric field. A high permittivity of ferroelectrics, which heavily depends on temperature, and spontaneous polarization leads to the existence of a considerable ECE that reaches the maximum values near the phase transition temperatures. Progress in the creation of a solid-state cooler is largely restrained by the absence of readily available materials having a large ECE. One of such possible materials is ceramic tiles based on barium titanate $BaTiO_3$, cheaper and simpler in manufacture than crystals.

Barium titanate is one of the most widespread ferroelectrics with a perovskite crystalline structure. The ferroelectric properties of $BaTiO_3$ were found already in 1944 at the Physical Institute named after P.N. Lebedev of the USSR AS by Vul and Goldman [4]. When temperature decreases, it undergoes 3 phase transitions: from the paraelectric cubic and ferroelectric tetragonal, then to the orthorhombic and, finally, to the rhombohedric phase. The crystalline $BaTiO_3$ near the phase transitions has a significant ECE up to 1.6 K at not very high voltages of 1 MV/m [5]. ECE for ceramics is somewhat smaller and is equal to 1.3 K at the voltage of 2 MV/m [6]. ECE is rather small at room temperatures, where barium titanate undergoes a phase transition from the tetragonal to orthorhombic phase. The greatest temperature change under ECE at this temperature range is about 4–5 times smaller than in the vicinity of the Curie–Weiss temperature. Thus, for the electric field of 2 MV/m the value of ΔT does not exceed 0.22 K as per the data of [7] and 0.1 K as per the data of [6,8,9].

Currently obtained films are usually polycrystalline and consist of granules with a size from tens of nanometer to tens of micrometers. According to the experimental studies conducted by means of X-ray or neutron radiation [10,11], each granule is surrounded by a transition layer approximately $\sim$1 nm and $\varepsilon \sim 100$ thick (dead layer, passive layer). The presence of a transition layer leads to a considerable

change in the ferroelectric properties. In particular, if the granule size is below a certain critical value, estimated at 10 nm for $BaTiO_3$, there is no spontaneous polarization in such ferroelectrics [10,12]. In addition to a dielectric layer, there are gaps (pores) between the granules, which are filled with gaseous medium that contains a mixture of air and plasticizer vapors. The presence of pores leads to a decreased ceramics density as compared to the density of monocrystalline $BaTiO_3$. The properties of comparatively thick films (thicker than 1 μm) do not depend on thickness [12], and the difference of films from ceramics can be described by means of boundary conditions [13]. Hereafter we will consider only ceramics as simpler ones to describe. In order to describe films, certain boundary conditions on the film surface should be simply added to the equations given below.

The study of micro- and nanocrystalline ceramics shows a strong dependence of their physical properties on synthesis conditions and grain size [6,8,9,12,14–16]. A change of synthesis temperature affects not only the grain sizes, but also on their shape, distribution, density of ceramics, porosity. The available experimental data shows that ferroelectric ceramics can be considered as a composite formed by granules (grains) coated with a dielectric and air shell placed in a matrix (four-phase composite model). A ball, a spheroid, or an ellipsoid can be considered as an inclusion form. The solution of the electrostatic problem for the spheroidal granule shape was found in [17] under a linear dependence of polarization on electric field. Explicit formulas for a non-linear Landau–Ginzburg (LG) model can be obtained only for an electric field parallel to a spheroid axis [18]. In theoretical developments, dependence on elastic deformations is usually absence or is assumed to be known [19]. A solution of the joint problem of elasticity and non-linear LG equation was obtained for the first time in this paper. Since the solution of the electrostatic problem was considered in sufficient detail in [18], the main attention is paid to impact of elasticity on ceramics properties. The theoretical research results are compared to the experimental ones obtained for the ceramics of barium titanate.

2. Theoretical model

2.1. Distribution function and physical model of the granule

We will model the ceramics by a set of ferroelectric balls. The ball radius is denoted as R. Each ball is coated with two layers with radii R_1 and R_2 $(R < R_1 < R_2)$ — with dielectric and air layers, and the latter takes into account the presence of pores between the granules (see Fig. 1). Many ferroelectric balls were placed in a dielectric matrix. Layer thickness for the considered ball with $h_1 = R_1 - R$, $h_2 = R_2 - R_1$ will be considered small as compared to radius R. Moreover, dielectric layer h_1 will be considered independent from R, which complies with

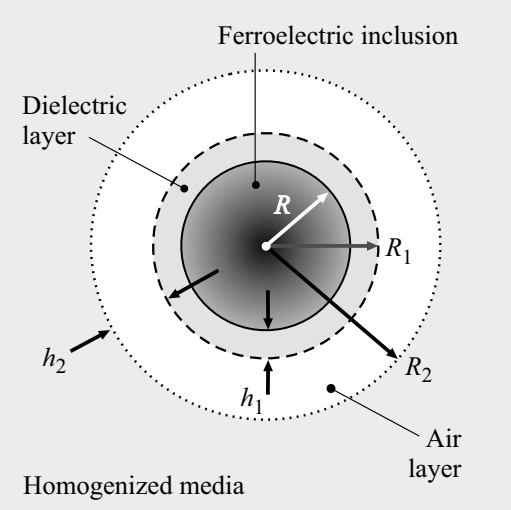

Figure 1. Four-phase model of a granule in ferroelectric ceramics.

the experimental data [10,11]. Dependence of air layer thickness on R will be determined according to relative depth ρ, where ρ is the ratio of ceramics density D to density of crystalline $BaTiO_3$ – D_{BTO}, $\rho = D/D_{BTO}$. Let us denote the ball volume as V_g, air volume as V_{air}, and the total volume as $V = V_g + V_{air}$. We will consider that the whole air volume is in the surface layers. The ceramics weight is a sum of the weight of balls with a dielectric shell, density of which matches the density of pure $BaTiO_3$, and the pore air weight which is neglected. The presence of air weight leads to a decrease of the ceramics density as compared to density $BaTiO_3$. The relative total ball volume matches the relative density $\rho = V_g/V$, while the relative total volume of air layers is equal to $V_{air}/V = 1 - \rho$. Assuming that all air is in an air layer, the equality for its thickness, from the elementary geometric considerations, is $h_2(R) = \frac{1-\rho}{3\rho} R$. Multiplier $1/3$ was obtained on condition of a constant radius for all granules. Let us show that this multiplier does not depend on the function of granule size distribution $w(R)$. On the premise that air layer thickness linearly depends on R, $h_2 = kR$, k — a certain proportionality coefficient, average volumes of granule $\bar{V}_g$ and air $\bar{V}_{air}$ are set by integrals

$$\bar{V}_g = \frac{4\pi}{3} \int_0^\infty w(R, L, \sigma) R^5 \mathrm{d}R,$$

$$\bar{V}_{air} = 4\pi k \int_0^\infty w(R, L, \sigma) R^5 \mathrm{d}R. \qquad (1)$$

Constant k is determined from the ratio $\frac{V_{air}}{V_g} = \frac{\bar{V}_{air}}{\bar{V}_g} = \frac{1-\rho}{\rho}$. From here $k = (1-\rho)/3\rho$, and this value does not depend on form of the distribution function.

Finding of the electric and elastic fields in ceramics requires knowledge of their behavior in a separate ball and the function of ball size distribution $w(R)$. Function $w(R)$ is assigned by granule distribution at the moment of baking start and by baking time. Without dwelling upon baking details (a separate paper will be dedicated to this process), we will assume that $w(R)$ is a normal distribution. More precisely, $w(R)$ will be considered as a spherically symmetrical three-dimensional normal distribution, since each granule has three dimensions (d_1, d_2, d_3). A three-dimensional distribution is obtained from a product of three normal one-dimensional distributions

$$w_0(d_i, L_i) = \frac{1}{\sqrt{2\pi}\sigma_i} \exp\left[-\frac{(d_i - L_i)^2}{2\sigma_i^2}\right], \quad i = 1, 2, 3 \quad (2)$$

where L_i — the most probable granule size along the x_i axis, σ_i — root-mean-square deviation from L_i. If we assume equality of the most probable dimensions $L_1 = L_2 = L_3 = L/\sqrt{3}$ and root-mean-square deviations $\sigma_1 = \sigma_2 = \sigma_3 = \sigma$, then after integration by angles in a spherical coordinate system defined in a conventional manner according to the Cartesian one (d_1, d_2, d_3), $\left(R = \sqrt{d_1^2 + d_2^2 + d_3^3}\right)$, we obtain an explicit expression for $w(R)$

$$w(R) \equiv w(R, L, \sigma) = \frac{2R}{\sqrt{2\pi}L\sigma R} \operatorname{sh}\left(\frac{RL}{\sigma^2}\right) \exp\left(-\frac{R^2 + L^2}{2\sigma^2}\right). \quad (3)$$

Hereafter $w(R)$ will mean an arbitrary distribution law, and $w(R, L, \sigma)$ — a three-dimensional normal distribution. The granule shape is an ellipsoid at values of mathematical expectations $L_{1,2,3}$ which differ from each other. Number of granules $N(R_{\min}, R_{\max})$ whose size meets the inequalities $R_{\min} < R < R_{\max}$, by definition of the distribution function is specified by an integral

$$N(R_{\min}, R_{\max}) = \int_{R_{\min}}^{R_{\max}} w(R, L, \sigma) R^2 \mathrm{d}R. \quad (4)$$

If the root-mean-square deviation is sufficiently small ($3\sigma < L$, the rule 3σ), the contribution of granules with radius $R < L - 3\sigma$ becomes negligible. In this case, a three-dimensional distribution can be replaced with a high accuracy degree by a one-dimensional one of the form (2). Mathematical expectation L and root-mean-square deviation σ are defined by baking time and temperature T_g. Parameters σ, L can be defined as per the experimental data. An increase of T_g causes an increase both of L and σ [6,8,9,12,14–16]. An initial distribution can be normal, and can be sufficiently arbitrary [20]. When baking time increases, the arbitrary distribution usually tend to the normal one. Thus, the initial distribution, which is a sum of two normal ones with the typical particle size of 80 and 200 nm, after 14 h of baking is close to the normal distribution with the average size of 252 nm [21]. A comparison with the experimental data shows that in some cases three-dimensional distribution (3) must be used [15], while in some cases its one-dimensional approximation of form (2) is sufficient. Distribution (3) as a more general one will be used subsequently.

2.2. Problem setting and main equations

Let us now describe a separate ball of radius R. We will study the field distribution in a single ball located in an external electric field $\mathbf{E}_{\text{ext}}$. This field at large distances from the ball is considered homogeneous and parallel to the applicate axis. It is assumed that, in addition to an electric field, hydrostatic pressure p acts from the side of neighboring balls. This pressure can be due to a mismatch of crystalline lattice parameters, presence of spontaneous deformation, electrostrictive effects in the matrix, difference of thermal expansion coefficients for the phases.

The electric and elastic fields will be described using electric potential φ, polarization P and elastic displacements u_i, $i = 1, 2, 3$. They are used to determine electric field intensity $\mathbf{E} = -\nabla\varphi$ and elastic stresses $u_{ij} = (u_{i,j} + u_{j,i})/2$. Hereinafter the index after the comma means differentiation by the corresponding variable. Hereafter we will assume that polarization and electric field in the ball are parallel to the external electric field, and can be considered as scalar quantities. Assuming this, the relationship of polarization and intensity in the ball is specified by a generalized Landau–Ginsburg equation [22]:

$$E = aP + bP^3 + cP^5 - 2P\left[q_{12}(u_{11} + u_{22}) + q_{11}u_{33}\right]. \quad (5)$$

Here a, b, c are LG coefficients, q_{ij} are electrostrictive coefficients. Thereat, only coefficient $a = a_0(T - T_{\text{CW}})$ depends on temperature T, where $a_0 = 1/\varepsilon_0 C$, T_{CW} — Curie–Weiss temperature, C — Curie constant and ε_0 is the electric constant. Equation (5) is true if polarization and electric field have the same direction. Its study requires finding of the deformation tensor values and electric field intensity according to the specified value of E_{ext}.

First we will write out the relation of the stress tensor σ_{ij} with the deformation tensor (the Hooke law) if electrostriction is present [22]:

$$\sigma_{11} = c_{11}u_{11} + c_{12}u_{22} + c_{12}u_{33} - q_{12}P^2, \quad (6a)$$

$$\sigma_{22} = c_{12}u_{11} + c_{11}u_{22} + c_{12}u_{33} - q_{12}P^2, \quad (6b)$$

$$\sigma_{33} = c_{12}u_{11} + c_{12}u_{22} + c_{11}u_{33} - q_{11}P^2, \quad (6c)$$

$$\sigma_{23} = 2c_{44}u_{23}, \quad \sigma_{13} = 2c_{44}u_{13}, \quad \sigma_{12} = 2c_{44}u_{12}, \quad (6d)$$

where c_{11}, c_{12}, c_{44} are elastic constants in the matrix (Voigt) notations. Hereafter we will restrict ourselves to the isotropic medium case when only 2 independent elastic constants are present. It should be noted that, terms $\beta(T - T_0)$, which define thermoelastic stresses, can be added to the right-hand member of ratio (6) for σ_{ii} in

order to refine the model. Here T_0 is temperature at which thermoelastic deformations are absent, while coefficient β is associated with thermal expansion coefficient α by ratio $\beta = -(c_{11} + 2c_{12})\alpha$. In addition to thermoelastic terms, deformations caused by a mismatch of crystalline lattices can be also taken into account. An important aspect is the fact that the thermoelastic terms inside the ball are constant quantities. We will restrict ourselves to the electrostrictive terms for a ball down, while for a matrix we will join the above-mentioned factors into hydrostatic pressure p.

The introduced quantities shall meet the standard equations of electrostatics and elasticity [23]:

$$\mathrm{div}(\varepsilon_0 E + P) = 0, \quad \sigma_{ij,j} = 0. \tag{7}$$

It immediately follows from this that electric field intensity E_3 and polarization P_3 in the ball are not only directed along the same axis, but are also constant. This makes it possible to consider the tasks of polarization and deformation determination independently of each other.

2.3. Approximate solution

Deformation homogeneity follows from the conjecture of polarization homogeneity in equations (6). Overall homogeneous deformation can be presented as a sum of homogeneous all-around (hydrostatic) extension (or compression) and homogeneous shear [24]. The presence of shear gives rise to additional components in the electric field and polarization, i.e. to violation of the conjecture of homogeneous polarization. Shear deformation is proportional to R^{-2} and, besides, its average value for the ball is 0 [24]. Due to this, this part of deformation can be neglected for microgranules ($R > 200$ nm) and only all-around compression can be considered. To do so, we will go to a spherical coordinate system (r, ϑ, φ) with the center at the ball beginning. Due to spherical symmetry both of the load and the system under study, the only non-zero component of the displacement vector will be the radial u_r. Thereat, the non-zero components of the deformation tensor have the form $u_{rr} = u_{r,r}, u_{\vartheta\vartheta} = u_{\varphi\varphi} = u_r/r$ [24]. Displacement u_r and σ_{rr} must be continuous on the interfaces (at $r = R$, R_1, R_2). The general solution of the elasticity equations in the case of hydrostatic forces has the form [24]:

$$u_r = B_1 r + B_2 \frac{1}{r^2}, \tag{8}$$

where $B_{1,2}$ are arbitrary constants. Since we have 4 media, there are 8 constants, 2 of which are found at once due to the requirement of displacement restriction in the ball center and at infinity. As a result we have 6 unknown quantities, for which we can write down a linear equation system resulting from the boundary conditions. Unfortunately, analysis of the obtained solution is hindered due to the awkwardness of the obtained expressions, therefore we will use the smallness of layer thicknesses and simplify the boundary conditions. This will be done using the matrix method [25], which makes it possible to disregard the thin layers and substitute them by approximate boundary conditions. Let us make a column X of quantities being continuous at interfaces of various media, $X = (u_r, \sigma_{rr})^{\mathrm{tr}}$. Symbol tr means transposition. Ratios (6) (at $P = 0$) and equations (7) in a spherical coordinate system are written over as [24]:

$$\sigma_{rr} = c_{11} u_{rr} + 2c_{12} \frac{u_r}{r}, \tag{9a}$$

$$\sigma_{\vartheta\vartheta} = \sigma_{\varphi\varphi} = c_{12} u_{rr} + (c_{11} + c_{12}) \frac{u_r}{r}, \tag{9b}$$

$$\frac{\mathrm{d}\sigma_{rr}}{\mathrm{d}r} + \frac{1}{r}(2\sigma_{rr} - \sigma_{\vartheta\vartheta} - \sigma_{\varphi\varphi}) = 0. \tag{9c}$$

Equations (9) yield and expression for the derivative of X with respect to r

$$\frac{\mathrm{d}X}{\mathrm{d}r} = MX,$$

$$M(r) \equiv \begin{pmatrix} -\dfrac{2c_{12}}{rc_{11}} & \dfrac{1}{c_{11}} \\ \dfrac{2}{r^2}\left(c_{11} + c_{12} - \dfrac{2c_{12}^2}{c_{11}}\right) & -\dfrac{2}{r}\left(1 - \dfrac{c_{12}}{c_{11}}\right) \end{pmatrix}. \tag{10}$$

Since function $X(r)$ is continuous and differentiable, its values at the boundaries of thin layers are related by an approximate equation

$$X(R_2) = \left(I + M_1(R)h_1 + M_2(R)h_2 + O(h_1^2 + h_2^2)\right) X(R). \tag{11}$$

Here I is a unity matrix sized 2×2, while matrix $M_1(r)$ has the form (10), where the values of the elastic constants were taken for the first layer, while matrix $M_2(r)$ includes only the elastic coefficients for the second layer. Change of coordinate r in layers is neglected. The more precise formulas containing $\int M_{1,2}(r)\mathrm{d}r$ are given in [18]. Equality (11) allows for disregarding both layers and substituting their influence by approximate boundary conditions, which are the more precise, the smaller the layer thickness. The terms, which give rise to a deformation, must be taken into account in order to write simplified boundary conditions. In a ball, this is the average value of electrostrictive terms $-\bar{q}P^2$, where $\bar{q} = (q_{11} + 2q_{12})/3$ is the average value of electrostrictive coefficients. Deformation in the matrix is caused by the presence of pressure p. By adding the specified quantities to quality (11), we obtain a boundary condition

$$X(R_2) = (I + M_1(R)h_1 + M_2(R)h_2)X(R) + F,$$

$$F = \begin{pmatrix} 0 \\ \bar{q}P^2 + p \end{pmatrix}. \tag{12}$$

Now, according to the general solution (8), we will find the displacement in the ball in the form $u_r = A^i r$, and in the matrix — in the form $u_r = A^m R^3/r^2$, where A^i and A^m are the desired quantities having the length unit. The superscript indicates that the quantity pertains to the inclusion (i) or

matrix (m). By substituting the specified expressions into the boundary conditions (12) and calculating σ_{rr}, we obtain a system for determination of constants $A^{i,m}$

$$A^m \begin{pmatrix} R \\ -3c_{11}^m + 2c_{12}^m \end{pmatrix} = A^i (I + M_1(R)h_1 + M_2(R)h_2) \begin{pmatrix} R \\ c_{11}^i + 2c_{12}^i \end{pmatrix} + F. \quad (13)$$

Despite the possibility to obtain a precise solution of system (13), let us write out an approximate solution obtained from the precise one by expansion in terms of small parameter $(h_1 + h_2)/R$

$$u_i = A^i r, \quad u_{rr} = u_{\vartheta\vartheta} = u_{\varphi\varphi} = A^i,$$

$$A^i = \left(A_0 + A_1 \frac{h_1}{R} + A_2 \frac{h_2}{R}\right)(p + \bar{q}P^2). \quad (14)$$

Constants A_j, $j = 0, 1, 2$ are determined only be the phases' elastic properties (matrix coefficients $M_1(R)$ and $M_2(R)$) and do not depend on radius R, for instance

$$A_0 = -\frac{1}{c_{11}^i + 2c_{12}^i + 2(c_{11}^m - c_{12}^m)}. \quad (15)$$

We will not write out the formulas for constants $A_{1,2}$ due to their awkwardness. It should be noted that A_1 comprises only the elastic constants of the inclusion, matrix and dielectric layer. It follows that coefficient A_1 little depends on conditions of ceramics making. On the contrary, coefficient A_2 is determined by air layer conditions which heavily depend on sintering conditions. The obtained values for displacement make it possible to find the deformation tensor components and obtain the following equation for polarization in the ball

$$E = \hat{a}P + \hat{b}P^3 + cP^5, \quad (16)$$

where modified LG coefficients $\hat{a}$, $\hat{b}$ have the form

$$\hat{a} = a - 2p(2q_{12} + q_{11})\left(A_0 + A_1\frac{h_1}{R} + A_2 k\right),$$

$$\hat{b} = b - 2\bar{q}(2q_{12} + q_{11})\left(A_0 + \frac{A_1}{R} + A_2 k\right). \quad (17)$$

Quantity $k = h_2/R = (1 - \rho)/3\rho$ is determined by relative ceramics density ρ. When solving the electrostatic problem, we obtain $E = \varkappa E_{\text{ext}}$, where coefficient $\varkappa$ is determined by the dielectric constants of the layers and matrix [18].

It follows from formula (17) that a change of LG coefficients $\hat{a} - a$ and $\hat{b} - b$ at a change of radius R is proportional to each other. It should be also noted that the initial equation for the ball ferroelectric material in the state equation contained only one temperature-dependent coefficient — a. Two coefficients in (16) should be considered as dependent on T for ceramics.

The following dependence of phase transition temperature T_{PT} on grain size follows from equation (16)

$$T_{\text{PT}} = T_{\text{CW}} - 2\varepsilon_0 C p(2q_{12} + q_{11})\left(A_0 + A_1\frac{h_1}{R} + A_2 k\right). \quad (18)$$

The main role in case of small (less than 200 nm) granule sizes in dependence (18) is played by the term proportional to R^{-1}. The result is inverse proportionality of T_{PT} to grain size [12]. Thereat, the proportionality coefficient little depends on ceramics synthesis conditions. The authors of [26], who studied ceramics $0.9\text{Pb}(\text{Mg}_{1/3}\text{Nb}_{2/3})_3{-}0.1\text{PbTi}_3$, found that T_{PT} has a maximum at a certain grain size. The presence of the maximum of T_{PT} for ceramic barium titanate was found in [27]. Existence of the phase transition temperature maximum can be explained within the framework of the suggested model. Extremeness of T_{PT} is associated with existence of roots of equation

$$A_1\frac{h_1}{R^2} = A_2\frac{\mathrm{d}k}{\mathrm{d}R}, \quad A_1\frac{h_1}{R^2} = -\frac{A_2}{3\rho^2}\frac{\mathrm{d}\rho}{\mathrm{d}R}, \quad (19)$$

i.e. with ceramics density behavior. The roots of equation (19) may exist if density decreases with increase in the average granule size, i.e. with increase of baking temperature T_{g}. Such a situation is possible at sufficiently high baking temperatures exceeding 1300°C. For instance, density of barium titanate ceramics in [6] has a vague maximum at $T_{\text{g}} = 1350$°C. Consequently, granules with the maximum phase transition temperature can form at $T_{\text{g}} > 1350$°C.

The obtained formulas make it possible to calculate the main characteristics of ceramics: polarization, permittivity, heat capacity, pyroelectric and electrocaloric coefficients, ECE. For instance, the average polarization value is determined using the formula

$$P = \int w(R, L, \sigma)P(R)\mathrm{d}R. \quad (20)$$

Here $P(R)$ is the average polarization in the ball B_2, which includes both layers. We obtain the following formula from (16) for local pyroelectric coefficient $\partial P/\partial T$ in the ferroelectric

$$\frac{\partial P}{\partial T} = \frac{\hat{a}_T P + \hat{b}_T P^3}{\hat{a} + 3\hat{b}P^2 + 5cP^4}, \quad (21)$$

where

$$\hat{a}_T = \frac{\mathrm{d}\hat{a}}{\mathrm{d}T}, \quad \hat{b}_T = \frac{\mathrm{d}\hat{b}}{\mathrm{d}T}. \quad (22)$$

are derivatives from the modified LG coefficients with respect to temperature. ECE for a single ball is found using the known pyroelectric coefficient by integration of the formula for local ECE over B_2 [3]

$$\mathrm{d}T = -\frac{T}{CV_2}\left(\int\limits_{B_2}\frac{\partial P}{\partial T}\mathrm{d}V\right)\mathrm{d}E. \quad (23)$$

Here C is heat capacity of the system (ball B_2), determined as a sum of heat capacities of the ball and the layers around it.

Equation (23) is written in the differential form. This equation in the integral form will be as follows

$$\Delta_R T = -\int_{E_1}^{E_2} \frac{T}{CV_2} \left(\int_{B_2} \Pi \mathrm{d}V \right) \mathrm{d}E. \qquad (24)$$

Here $\Delta_R T$ is a temperature change in a separate granule of radius R, caused by an electric field change from value E_1 to value E_2. Change of the temperature of entire sample ΔT for the random law of granule size distribution $w(R)$ is written as

$$\Delta T = -\int_R \int_{E_1}^{E_2} \frac{T}{CV_2} \left(\int_{B_2} \Pi \mathrm{d}V \right) w(R) \mathrm{d}E \, \mathrm{d}R. \qquad (25)$$

It should be noted that, as compared to the known ECE formulas [3], equations (23), (24) included an additional integration over the granule volume, while the main ECE formula (25) also includes integration over granule size R. Formula (25) is universal and does not depend on the form of distribution law $w(R)$ and pyroelectric coefficient Π.

Thus, the function of granule size distribution $w(R)$, pyroelectric coefficient Π and granule heat capacity C must be known in order to find the ceramics temperature change at a change in the electric field. Granule heat capacity is easily determined using the known heat capacities of barium titanate/air and relative density value ρ which is determined experimentally. The normal distribution $w(R, L, \sigma)$ (3), where average granule size L and root-mean-square deviation σ can be easily determined according to the experimental data, can be chosen as a distribution function. The main difficulty is in the fining of pyroelectric coefficient Π, which is determined using the above-mentioned four-phase model. Quantity Π is determined by elastic and electric properties of the ferroelectric core (ball), dielectric and air layers and their geometrical parameters. These properties for barium titanate and air are known [22]. Air layer thickness is set by relative density ρ. The dielectric layer is studied much more poorly. The main problem is to find the temperature dependence of its permittivity, since the small layer thickness hinders the separation of its properties from the core properties. Due to this, the present paper uses a conjecture that the dielectric layer properties do not depend on temperature, which may lead to a considerable different between theoretical and experimentally obtained dependences.

The only characteristic that cannot be obtained from state equation (16) is conductivity, behavior of which is usually described within the framework of the Heywang theory [28]. Conductivity depends rather heavily on properties of transition layers between granules, therefore, an explanation of its properties requires refining of the dielectric and air layer model by including a charge distribution into it.

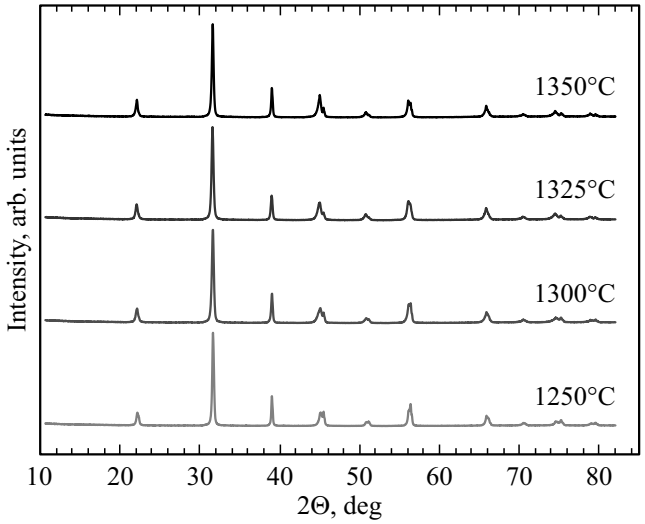

Figure 2. X-ray diffraction spectra of the points barium titanate samples at room temperature.

3. Experimental measurements

A series of experiments with barium titanate ceramics was conducted to study the dependence of ferroelectric properties on baking temperature. Samples were made by high-temperature sintering. Synthesis was performed in 2 stages (two-step sintering): titanium dioxide and barium carbonate were initially ground and mixed, and then long-term baking was carried out at a temperature sufficient for an active reaction between the components' solid phases (1200°C for two hours), then the obtained powders were ground and mixed again. The obtained charges were mixed with an organic plasticizer (acryl resin-based varnish), placed in a press mold and pressed at the pressure of 100 MPa, internal diameter of the press molds was 12 mm. Then the uncured blanks were synthesized at a high temperature, while the obtained ceramic samples were thinned to the thickness of 500 μm. Electrodes, made by burning-in of conducting silver-palladium paste, were applied on the polished surface of the made samples. Temperature change rate in the furnace at all synthesis stages did not exceed 0.07 K/s. The heating program during baking of uncured blanks provided for heating rate reduction to 0.03 K/s at temperatures of 500−700°C to minimize the ceramics density decrease due to intensive evaporation of the plasticizer. Final baking time varied within 1 to 3 h, while temperature T_g varied from 1200°C to 1400°C.

The phase composition of the made samples was studied by X-ray structural analysis. Fig. 2 shows the comparative X-ray diffraction spectra of barium titanate samples baked at different temperatures. The obtained spectra corresponds to the barium titanate spectrum in the tetragonal phase. The difference in the electrophysical properties of barium titanate, baked at different temperatures, was explained in [29] by a different phase composition. The performed X-ray studies did not reveal phase composition differences

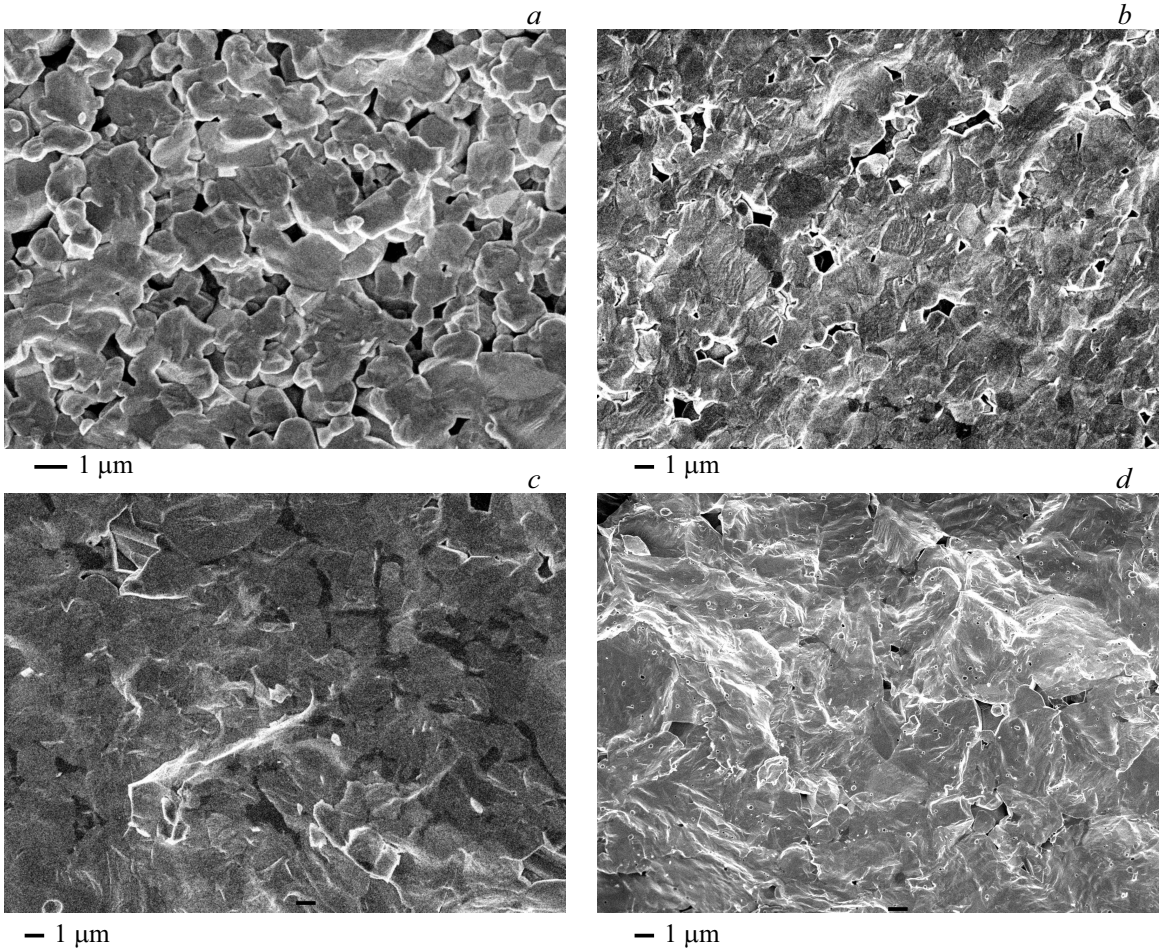

Figure 3. Microstructure analysis of the barium titanate ceramics samples annealed at $T_g = (a)$ 1250°C, (b) 1300°C, (c) 1325°C and (d) 1350°C.

of the samples synthesized at temperatures starting from 1325°C, consequently, it is more probable that the difference in electrophysical properties is associated with the sample microstructure, with grain size in particular.

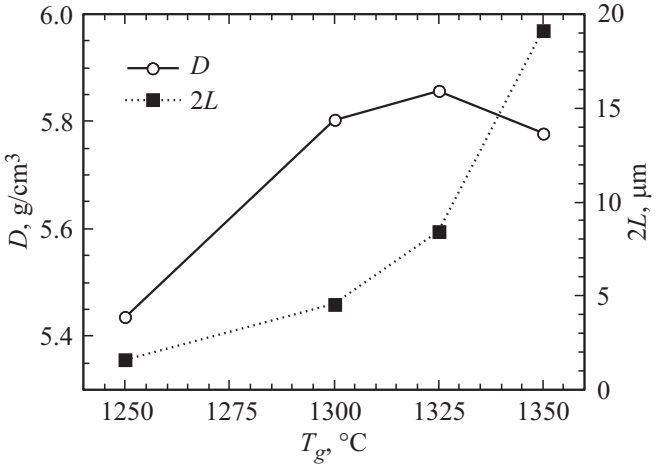

Figure 4. Dependence of density D and average grain size L on baking temperature of synthesis T_g.

The images of the sample chip obtained by scanning electron microscopy are shown in Fig. 3. The average granule sizes varied from 2 to 33 μm. Density of ceramic samples D was determined by hydrostatic weighing using a PX-224 OHAUS Pioneer laboratory balance. Apparent density was determined by hydrostatic weighing of freshly split fragments of ceramic material samples preliminarily saturated with liquid. For saturation by boiling, the samples were dried in a drying cabinet at 115 ± 5°C till reaching a constant weight. Hydrostatic weighing of the samples after boiling was performed in distilled water. The obtained experimental dependences of L and results of ceramics density measurement at different baking temperatures of synthesis are shown in Fig. 4.

The electrophysical and thermophysical properties of the made samples were studied. Temperature dependences of permittivity and dielectric loss angle tangent $\varepsilon(E, T)$, $\tan\delta(E, T)$ were measured using an Agilent E4980A digital immitance meter. Temperature measurement conditions were set using a Julabo 32 ME thermostat. Capacitance was the directly measured quantity. The error of its measurement within the used measurement limits was less than 0.1 pF,

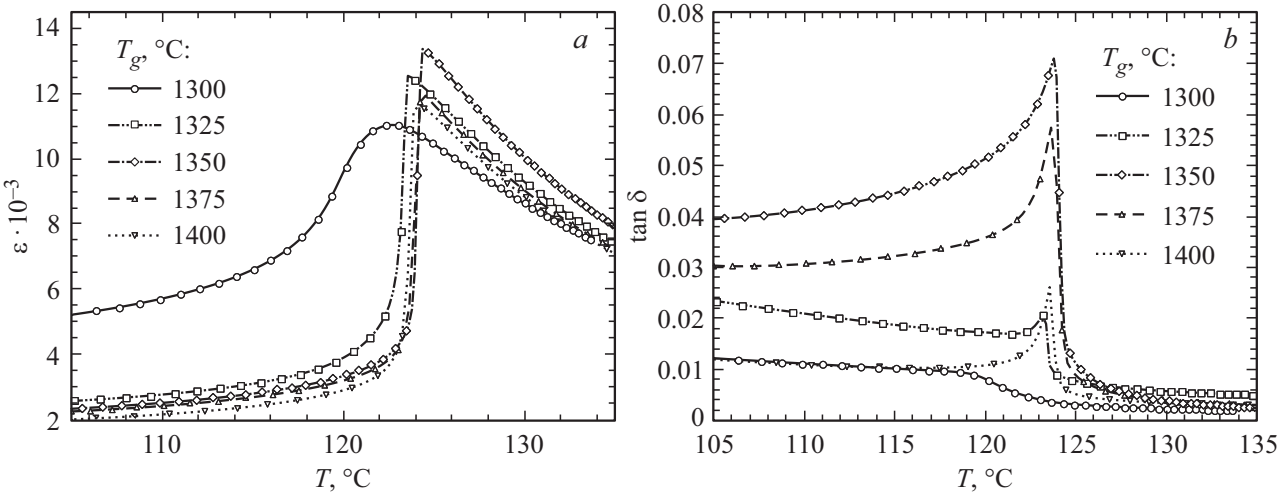

Figure 5. Temperature dependence (a) of permittivity ε and (b) dielectric losses $\tan\delta$ for different temperatures T_g.

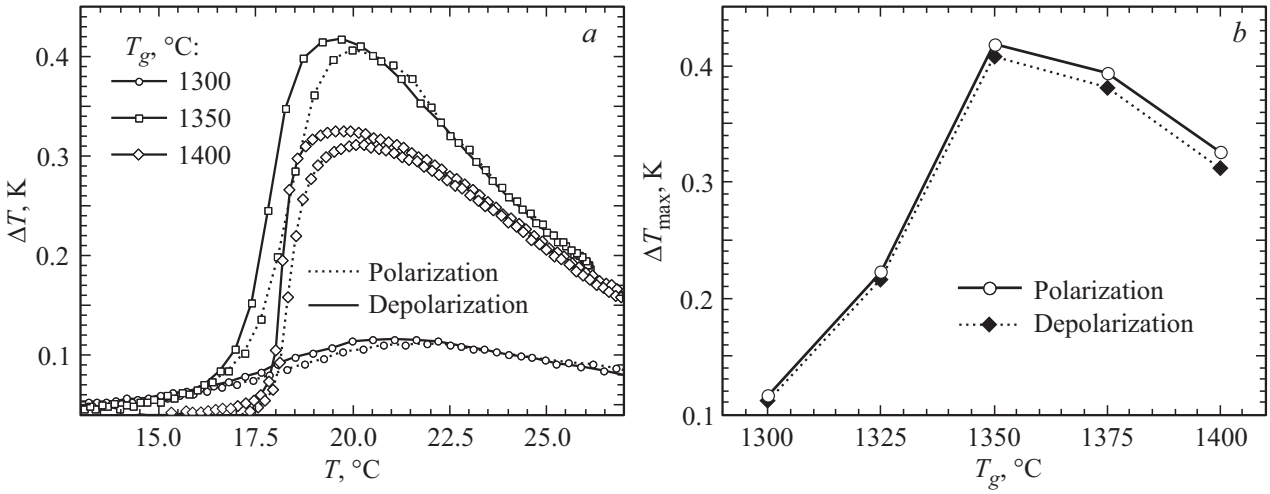

Figure 6. (a) Dependence of temperature change ΔT under the electrocaloric effect on temperature T for samples annealed under different conditions T_g. (b) Dependence of the largest temperature change ΔT_{max} under ECE on baking temperature of synthesis.

relative measurement error was 0.05%. The measurement signal was a signal with the amplitude of 1V. Due to the rather remarkable permittivity dispersion, typical for ferroelectric materials, measurements were performed at different sine signal frequencies in the range of 100 Hz to 1 MHz. The results of permittivity measurements are shown in Fig. 5, *a*. Fig. 5, *b* shows the dependence of dielectric losses on temperature.

Temperature, field and frequency dependences of the electrocaloric effect were measured by direct measurements of adiabatic temperature change using M213 Pt-100 precision platinum thermoresistive transducers. Temperature measurement accuracy was ± 2 mK. Measurements were performed near the phase transition between the tetragonal and rhombohedral phases, i.e. at nearly room temperatures. Dependence of temperature change ΔT under ECE is shown in Fig. 6. The differences in dependence ΔT for polarization and depolarization processes are due to pyro currents [30].

4. Discussion

Physical processes during baking of ceramics are described as follows. The initial power consists of granules in the ball shape with pores between them. As synthesis temperature increases, both the average and the largest granule size increase. This results in a decrease of grain surface area. When baking temperature is above 1300°C, the properties of ceramics begin changing abruptly. Ceramics density at 1325°C takes on the largest value (Fig. 2). The greatest change in granule size occurs in the interval from 1300°C to 1350°C. A similar effect of granule growth rate change in the given temperature range was observed in [6,16]. ECE increases considerably at that. Thus, ECE

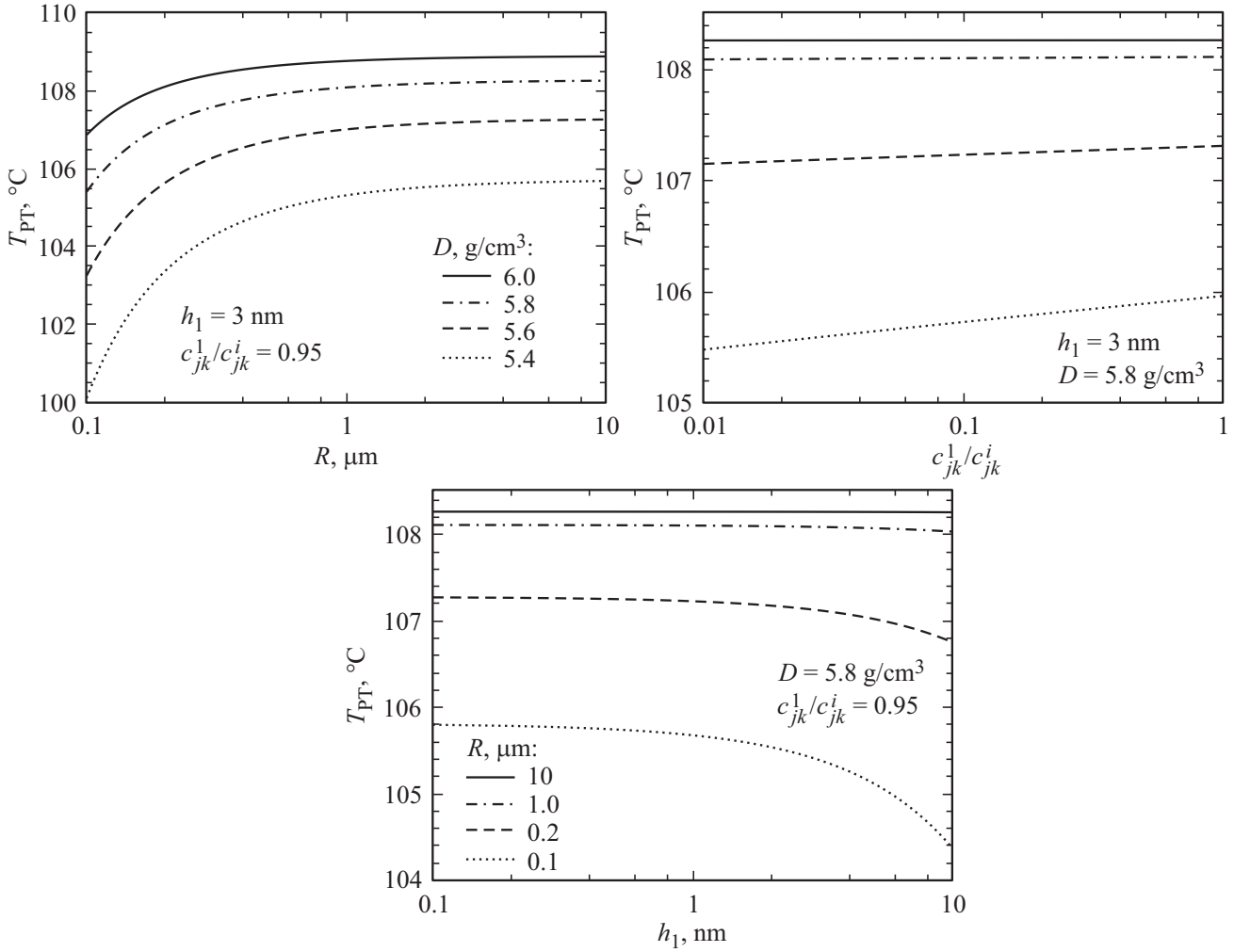

Figure 7. Dependence of phase transition temperature on granule size at different values of density (a), elastic properties (b) and dielectric layer thickness for different granule sizes (c).

for ceramics annealed at 1350°C is 4 times greater than for ceramics with T_g=1300°C (Fig. 6). Permittivity ε and losses ($\tan\delta$) also increase (Fig. 5). A similar phenomenon was noted in [6] and was associated with a change (at 1320°C) of the asymmetry sign for the granule size distribution. This means that the number of granules with sizes, exceeding the mathematical expectation, at $T > 1320$°C exceeds the number of smaller granules. According to the above-mentioned theory, permittivity and ECE increase with granule size increase. Phase transition temperature T_{PT} according to formula (18) is also a monotonically increasing function both of granule size and ceramics density (Fig. 7, a). It should be compared that, as compared to the experimental data, not only a granule size change, but also ceramics density must be taken into account. Influence of the dielectric layer properties was estimated by plotting dependences of temperature T_{PT} on values of elasticity coefficients (Fig. 7, b) and dielectric layer thickness (Fig. 7, c). Elastic constants of the dielectric layer c^1_{jk} in numerical calculations were taken as proportional to the ball elastic coefficients c^i_{jk}. The obtained dependences unambiguously show that phase transition temperature for ceramics with a granule size over 1μm is virtually independent both from elastic properties and thickness of the dielectric layer. Impact of dielectric layer on T_{PT} becomes noticeable only for granules with $R < 0.5\,\mu$m.

A decrease of ceramics density, according to equation (19), may give rise to a maximum of the dependence of phase transition temperature in ceramics T_{PT} on baking temperature of synthesis. This assumption was checked by plotting T_{PT} and temperature of permittivity maximum T_m vs. T_g (Fig. 8). The dependence $T_{PT}(T_g)$ was found according to temperature dependence ε based on the Curie law. We also give (for comparison) the results of calculation of T_{PT} based on (18) within the framework of the four-phase model using the data from [22]. The maximum value of T_{PT} is achieved at 1350°C in full compliance with the theory. The maximum of T_{PT} exists due to the air layer properties and, consequently, is unstable with respect to changing conditions of ceramics synthesis.

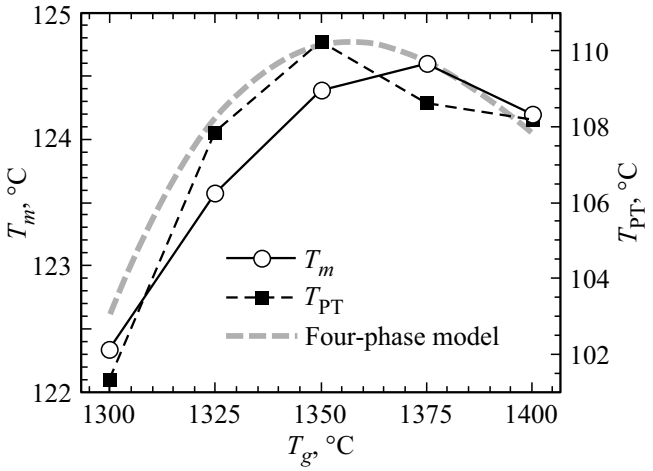

Figure 8. Dependence of temperature of the maximum of permittivity T_m and phase transition temperature T_{PT} on baking temperature of synthesis. The dashed line shows the results of the four-phase model for T_{PT}.

The highest values of permittivity and phase transition temperature, as well as the largest ECE at room temperatures were obtained for ceramics with $T_g = 1350°C$. The above-mentioned quantities for ceramics with other baking temperatures behave independently from each other (see Fig. 5, 6, 8). The absence of a strong correlation between permittivity and ECE is due to the fact that ECE is determined by a derivative of polarization with respect to temperature (pyroelectric coefficient Π). Nevertheless, these quantities are related, since a permittivity increase leads to a polarization increase and, consequently, to an increase of Π. When baking temperature of synthesis rises above 1350°C (1365°C according to [6]), ECE and permittivity decrease. We think that this is associated with two circumstances. With 1350−1365°C the granule distribution has a small dispersion. An increase of temperature or baking time of synthesis leads to an increase of dispersion due to the diffusion nature of the baking process [31]. Grain size distribution becomes less and less δ-shaped and approaches a uniform distribution. For the average grain size of 25 μm there is a certain number of grains sized 50 μm and a certain number of grains sized less than 200 nm. Phase transition temperature for grains of the extreme sizes differs by 20°C and more. This results in blurring of the sharp peak of ECE dependence on temperature. A similar explanation is given for the „flattening“ of the temperature dependence of permittivity and the decrease of its maximum value. Moreover, the grain surface area decreases, but the pore volume does not decrease. This means that transition layer's properties become closer to pore properties. Its permittivity and ECE decrease. The two mentioned circumstances cause the maxima of permittivity and ECE in case of a certain granule size.

5. Conclusion

The paper suggests considering the ceramics as a composite medium where the inclusions have the shape of a ball coated with a dielectric and air shell (four-phase medium). The properties of an air layer, which models the ceramics pores, to a great extent depend on synthesis conditions. On the contrary, the properties of the dielectric layer are almost unchanged. We have managed to solve (on the assumption of polarization homogeneity) the elastic problem for a single granule and to find the coefficients in the Landau–Ginzburg equation. Consideration of elasticity leads to radius-dependent terms in the LG coefficients. A change in coefficient a is proportional to pressure p with which the neighbors act on the given granule. The experimentally revealed law of Curie–Weiss temperature decrease with granule size decrease, and the existence of a maximum in the dependence of phase transition temperature on granule size follow from the difference of coefficients a and $\hat{a}$. The constant which governs the Curie–Weiss temperature decrease law is mainly determined by the dielectric layer properties and is therefore little dependent on experiment conditions. Presence of baking temperature T_g, at which the Curie–Weiss temperature has a maximum, is determined by properties of the air layer which is rather sensitive to quality of the initial powder and baking conditions. Due to this, the said effect is unstable and cannot always manifest itself. The presence of radius-dependent terms in coefficient $\tilde{b}$, which arise due to electrostriction, makes it possible to explain the change in phase transition temperatures between tetragonal, orthorhombic and rhombohedral phases. As distinct from the phase transition temperature between the cubic and tetragonal phases (Curie–Weiss), these temperatures can decrease with granule size increase [32]. This phenomenon cannot be explained within the framework of the standard model [19], where only coefficient $\hat{a}$ depends on granule size.

An important role in electric and thermodynamic properties of ferroelectric ceramics is played by the function of grain size distribution and transition layer properties in which the presence of pores is taken into account. Grains of approximately similar sizes should be obtained in order to get the highest value of ECE magnitude. The experimentally obtained maximum ECE value for barium titanate ceramics at room temperature, equal to 0.42 K, exceeds the previously known ones [6–9]. This result shows the advantage of the two-stage synthesis method. Increase of synthesis temperature T_g from 1300 to 1350°C leads to a 4-fold increase of ECE ΔT, and the average granule size increases in approximately the same proportion. Further increase of T_g leads to ECE decrease, but the average granule size increases. It means that there is an optimal granule size at which ECE reaches the maximum value. The developed theory also indicates the existence of such a size. Unfortunately, the optimal granule size heavily depends on initial size of powder granules and on synthesis conditions. It can be stated with certainty

that nanogranule films ($40\,\text{nm} < L < 1\,\mu\text{m}$) have a smaller ECE than microgranule ones ($L > 1\,\mu\text{m}$), and the optimal grain size value may vary from several to tens of microns. The largest ECE in this paper was observed for ceramics with a granule size $L \approx 10\,\mu\text{m}$. It can be concluded that commercial multilayer ceramic capacitors cannot be used in cooling devices, since their granule size was chosen to obtain the best controllability or the highest permittivity ($L \sim 1\mu\text{m}$). The experimental data of this paper clearly shows a strong dependence of thermal and electric properties of ferroelectric ceramics on synthesis temperature and time. The developed theoretical model describes these properties quantitively and can be used for ECE optimization and creation of a high-efficiency solid-state cooler.

Funding

The study was supported by a grant from the Russian Science Foundation (project No. 19-79-10074).

The electron microscopic studies were performed using the equipment of the federal Common Research Center „Materials Science and Diagnostics in Advanced Technologies“, supported by the Ministry of Education and Science of Russia.

Conflict of interest

The authors declare that they have no conflict of interest.

References

[1] A.S. Sigov, E.D. Mishina, V.M. Mukhortov. FTT **52**, *4*, 709 (2010) (in Russian).
[2] A. Starkov, O. Pakhomov, I. Starkov. Ferroelectrics **430**, *1*, 108 (2012).
[3] S. Karmanenko, A. Semenov, A. Dedyk, A. Es'kov, A. Ivanov, P. Beliavskiy, Yu. Pavlova, A. Nikitin, I. Starkov, A. Starkov, O. Pakhomov. New Approaches to Electrocaloric-Based Multilayer Cooling. In the book *Electrocaloric Materials*. Springer, Berlin Heidelberg (2014) Ch. VIII, P. 183–223.
[4] B.M. Vul, I.M. Goldman. Compt. Rend. Acad. Sci. URSS **49**, 177 (1945).
[5] Y. Bai, K. Ding, G.P. Zheng, S.Q. Shi, L. Qiao. Phys. Status Solidi A **209**, *5*, 941 (2012).
[6] B.C. Kim, K.W. Chae, C.I Cheon. J. Korean Phys. Soc. **76**, *3*, 226 (2020).
[7] X.C. Ren, W.L. Nie, Y. Bai, L.J. Qiao. Eur. Phy. J. B **88**, *9*, 1 (2015).
[8] A.V. Kartashev, V.S. Bondarev, I.N. Flyorov, M.V. Gorev, E.I. Pogoreltsev, A.V. Shabanov, M.S. Molokeev, S. Guillemet-Fritsch, I.P. Rayevsky. FTT **61**, *6*, 1128 (2019) (in Russian).
[9] S. Patel, M. Kumar. AIP Advances **10**, *8*, 085302 (2020).
[10] M.T. Buscaglia, M. Viviani, V. Buscaglia, L. Mitoseriu, A. Testino, P. Nanni, Z. Zhao, M. Nygren, C. Harnagea, D. Piazza, C. Galassi. Phys. Rev. B **73**, 064114 (2006).
[11] T. Hoshina, S. Wada, Y. Kuroiwa, T. Tsurumi. Appl. Phys. Lett. **93**, 192914 (2008).
[12] B.A. Strukov, S.T. Davitadze, S.G. Shulman, B.V Goltzman, V.V. Lemanov. Ferroelectrics **301**, *1*, 157 (2004).
[13] N.A. Pertsev, A.G. Zembilgotov, A.K. Tagantsev. Phys. Rev. Lett. **80**, *9*, 1988 (1998).
[14] P. Zheng, J.L. Zhang, Y.Q. Tan, C.L. Wang. Acta Mater. **60**, *13-14*, 5022 (2012).
[15] M.V. Zdorovets, A.L. Kozlovskiy. Vacuum **168**, 108838 (2019).
[16] O.V. Malyshkina, G.S. Shishkov, A.A. Martyanov, A.I. Ivanova. Mod. Electron. Mater. **6**, 141 (2020).
[17] O.G. Vendik, N.Yu. Medvedeva, S.P. Zubko. PZhTF **34**, *8*, 13 (2008) (in Russian).
[18] A.S. Starkov, I.A. Starkov, A.I. Dedyk, G. Suchaneck, G. Gerlach. Phys. Status Solidi B **255**, *2*, 1700245 (2018).
[19] J.H. Qiu, Q. Jiang. J. Appl. Phys. **105**, *3*, 034110 (2009).
[20] L. Wu, M.C. Chure, K.K. Wu, W.C. Chang, M.J. Yang, W.K. Liu, M.J. Wu. Ceram. Int. **35**, *3*, 957 (2009).
[21] Q. Jin, B. Cui, X. Zhang, J. Wang. J. Electron. Mater. **50**, *1*, 325 (2021).
[22] P. Marton, I. Rychetsky, J. Hlinka. Phys. Rev. B **81**, *14*, 144125 (2010).
[23] J. Nye. Physical properties of crystals, their representation by tensors and matrices. Izd-vo IL, M. (1960). 377 p. (in Russian).
[24] L.D. Landau, E.M. Lifshitz. Teoriya uprugosti. Nauka, M. (1987) (in Russian).
[25] A.S. Starkov, I.A. Starkov. ZhETF **146**, *5*, 980 (2014) (in Russian).
[26] M. Vrabelj, H. Uršič, Z. Kutnjak, B. Rožič, S. Drnovšek, A. Benčan, V. Bobnar, L. Fulanovič, B. Malič. J. Eur. Ceram. Soc. **36**, 75 (2016).
[27] S. Hu, C. Luo, P. Li, J. Hu, G. Li, H. Jiang, W. Zhang. J. Mater. Sci. Mater. El. **28**, *13*, 9322 (2017).
[28] W. Heywang. J. Mater. Sci. **6**, 1214 (1971).
[29] N. Funsueb, A. Limpichaipanit, A. Ngamjarurojana. J. Phys.: Conf. Ser. **1144**, *1*, 012133 (2018).
[30] A. Starkov, I. Starkov, Ferroelectrics **461**, *1*, 50 (2014).
[31] L.D. Landau, E.M. Lifshitz. Gidrodinamika. Nauka, M. (1986) (in Russian).
[32] X.H. Wang, I.W. Chen, X.Y. Deng, Y.D. Wang, L.T. Li. J. Adv. Ceram. **4**, *1*, 1 (2015).